Applied Physics Letters

Comparison of carrier-recombination in Ga(As,Bi)/Ga(N,As)-type-II quantum wells and W-type heterostructures

Cite as: Appl. Phys. Lett. **118**, 052103 (2021); https://doi.org/10.1063/5.0036073
Submitted: 02 November 2020 • Accepted: 20 January 2021 • Published Online: 02 February 2021

Julian Veletas, Thilo Hepp, Florian Dobener, et al.

Applied Physics Letters ARTICLE scitation.org/journal/apl

Comparison of carrier-recombination in Ga(As,Bi)/Ga(N,As)-type-II quantum wells and W-type heterostructures

Cite as: Appl. Phys. Lett. **118**, 052103 (2021); doi: 10.1063/5.0036073
Submitted: 2 November 2020 · Accepted: 20 January 2021 ·
Published Online: 2 February 2021

Julian Veletas,[1,a)] Thilo Hepp,[2] Florian Dobener,[1] Kerstin Volz,[2] and Sangam Chatterjee[1]

AFFILIATIONS

[1]Institute of Experimental Physics I and Center for Materials Research, Justus-Liebig-University Giessen, Heinrich-Buff-Ring 16, 35392 Giessen, Germany
[2]Faculty of Physics and Materials Sciences Center, Philipps-Universität Marburg, Hans-Meerwein-Str. 6, 35035 Marburg, Germany

[a)]**Author to whom correspondence should be addressed:** julian.veletas@exp1.physik.uni-giessen.de

ABSTRACT

The realization of efficient semiconductor lasers on GaAs substrates operating at 1.55 μm and beyond remains a technological challenge. As a potential solution, epitaxial heterostructures with type-II band alignment are currently discussed as an active region. Each individual layer in such heterostructures features a comparably large bandgap energy; therefore, spurious effects in laser operation such as reabsorption, multi-photon absorption, or Auger scattering are expected to be suppressed. The actual laser operation occurs across the internal interfaces as the electron and hole wave functions have their extrema in adjacent layers. Hence, a large wave-function overlap is key for efficient recombination. A direct comparison of symmetric and asymmetric Ga(N,As)/Ga(As,Bi) type-II quantum well heterostructures reveals that the symmetry of the layer arrangement drastically influences the charge-carrier recombination: disorder in the Ga(As,Bi) layer has more prominent effects for the asymmetric configuration compared to the symmetric one. The temperature dependence of the emission energy is mainly influenced by the Ga(N,As)-electron layers, while the temperature dependence of the full width at half maximum and the excitation dependence of the emission energy are dominated by the Ga(As,Bi)-hole layers. Photoluminescence excitation spectroscopy reveals the corresponding carrier-relaxation paths to the type-II transition.

Conventional near- and mid-infrared lasers on the InP or the GaSb platforms suffer from intrinsic loss channels such as Auger recombination or carrier leakage.[1–3] One approach to reduce such detrimental losses significantly and, additionally, migrating these infrared light emitting devices onto GaAs substrates is using a sequence of spatially indirect (type-II) transition between adjacent layers.[4,5] Such type-II heterostructures serve as active regions in infrared laser structures. They provide vast flexibility in an emission energy design by variation of the elemental composition. For example, Ga(N,As) and Ga(As,Bi) layers may act as electron quantum wells (QWs) and hole QWs, respectively. Recently, dilute Bi-containing semiconductors are gaining increasing interest[6–10] since the incorporation of bismuth into GaAs results in a rapid decrease in the bandgap.[11–14] In a band anti-crossing picture where the isoelectronic Bi level interacts with the upper valence bands (VBs) associated with GaAs, this shift is predominantly weighted on them.[15–17] Nitrogen atoms, on the other hand, induce a large shift of the conduction band (CB) if incorporated into GaAs, again decreasing the bandgap of the GaAs host.[18–20] These specific attributes of the type-I QWs lead to a flexible design regarding the type-II emission since band-offsets can, therefore, be tuned independently. Furthermore, the pseudomorphic growth of Ga(N,As)/[Ga(As,Bi)] leads to a tensile (compressive) strained layer on GaAs. This offers the possibility for strain-balanced heterostructures on GaAs substrates.[21]

Here, we perform early stage investigations on such type-II structures that are desired for use as active medium in surface emitting lasers. Temperature-dependent photoluminescence (PL) spectroscopy provides access to the fundamental emission properties of III–V semiconductors. Additionally, the temperature dependencies reveal disorder effects and, thus, enable in-depth studies on localized states of the structures constituents. Additionally, excitation-density-dependent PL data provide information on state filling effects and tail states. Photoluminescence excitation spectroscopy (PLE) as an absorption-like technique not only provides information on oscillator strength but also traces the carrier recombination paths of the type-II transition.

The samples are mounted in a helium-flow cryostat enabling temperature-dependent measurements from 4 K up to 400 K; this includes the range of operation temperatures of many 10s °C common to diode lasers. The sample's photoluminescence (PL) is imaged onto the 500 μm entrance slit of a 1 m Czerny-Turner spectrometer and is detected by a liquid-nitrogen cooled germanium detector using the phase sensitive line-scan lock-in technique. The system yields a spectral resolution of 2 nm. For the PL experiments, a diode-pumped continuous-wave intracavity frequency-doubled Nd:YAG laser excites the sample at 2.33 eV (532 nm). The excitation light is mechanically chopped at 109 Hz; its intensity is controlled using reflective neutral-density filters. A maximum excitation density of 11.3 kW/cm^2 is estimated on the sample. For the PLE experiments, a spectrally filtered super continuum source provides the tunable excitation. A 0.25 m Czerny-Turner-type monochromator defines a bandpass of 5 nm. The raw PLE data are corrected regarding different excitation densities due to the nonlinear emission of the super-continuum laser and the nonlinear optical response of the spectrograph.

All samples are grown in an Aixtron AIX200-GFR-MOVPE reactor and the structural parameters are verified by X-ray diffraction (XRD). The used precursors are triethylgallium (TEGa), tertiarybutylarsine (TBAs), unsymmetrical dimethylhydrazine (UDMHy), and trimethylbismuth (TMBi). A GaAs buffer layer is grown on a semi-insulating GaAs substrate to achieve a flat and reproducible surface for all samples. The asymmetric type-II sample consists of 3× Ga(N,As)/Ga(As,Bi) layers, while for the symmetric type-II sample, a second Ga(N,As) layer is introduced before the Ga(As,Bi) layer. This results in a 3× Ga(N,As)/Ga(As,Bi)/Ga(N,As) heterostructure, which is also referred to as the W-type structure. The thickness of the Ga(N,As) layer in the asymmetric Ga(N,As)/Ga(As,Bi) structure is 8 nm, while all other layers' thicknesses are 4 nm. The N or Bi fractions are 1.1% and 4.0%, respectively. Each of these stacks is capped by a thin, roughly 50 nm wide GaAs layer.

Figure 1 provides an overview of the characteristic spectral emission signatures of all samples. The normalized PL spectra (the scale factors are given next to the respective curves) at 300 K show two distinct peaks: the most pronounced luminescence feature is found at energies below the GaAs-related emission at 1.42 eV. Both the emission energies and the spectral line shapes of the Ga(N,As) and Ga(As,Bi) reference samples differ significantly. The emission from the Ga(As,Bi) reference shows strong inhomogeneous broadening and an exponentially decaying low-energy tail (blue line). This is due to extended tail states due to microscopic composition fluctuations (alloy disorder) as well as Bi clusters.[22,23] The PL from the Ga(N,As) reference sample (red line) is distinctly narrower and its low energy tail is much steeper. The PL of both the type-II sample and the W-type sample has its maximum at approximately 1.1 eV. The relative intensities of the room temperature emission are in agreement with our expectations: the type-I structures show higher intensities than the type-II structures, since they have higher oscillator strengths. The Ga(As,Bi) QW sample shows more inhomogeneous broadening and, hence, slightly lower intensities in comparison to the Ga(N,As) reference structure. The lack of wave-function overlap of electrons and holes in the spatially indirect arrangements explains the lower intensities of the type-II specimens. A direct comparison of the symmetric and asymmetric type-II structures indicates a higher overlap of electron and hole wave function in the symmetric heterostructures, which leads to

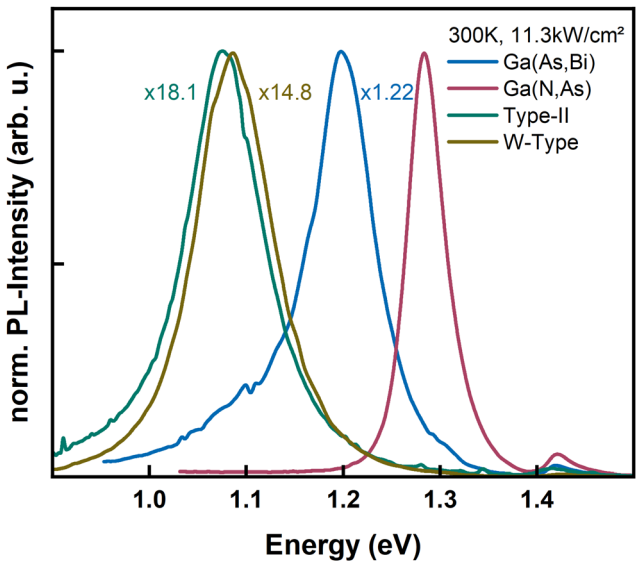

FIG. 1. PL spectra of all samples at 300 K.

higher PL-intensities. The line shape of both spatially indirect transitions inherits characteristics from the Ga(N,As) and the Ga(As,Bi) photoluminescence properties, while the actual line shapes of the type-II and the W-type samples differ slightly. We perform a detailed disorder analysis and investigate state filling and potential relaxation paths to get more insight in emission and relaxation properties.

Temperature-dependent PL measurements can reveal a so-called S-shape behavior in disordered type-I quantum well samples[24–26] as disorder affects their emission properties. Commonly, both the PL maximum, its full width half maximum, and its decay dynamics are affected.[27–29]

The PL-maximum energy shows a characteristic nonmonotonic behavior in energy with increasing temperature. A typical S-shape is observed, which is ascribed to thermally activated hopping processes of carriers between localized (tail-) states. This behavior is highly affected by the excitation density and is most pronounced for the lowest excitation density where least states are filled.[30] Here, excitation fluxes of 1.4 kW/cm^2 enable a full temperature-range analysis. Figure 2(a) displays the experimentally determined PL-maxima of all samples. The data are plotted as the colored squares, while the black lines act as guides to the eye. Here, the Ga(As,Bi) QW sample (blue rectangles) shows a broad disorder-related S-shape having its minimum at approximately 150 K (indicated by the blue dashed line). The local minima are reached for temperatures ranging from 50 K up to 200 K. In comparison, the Ga(N,As) QW sample's PL-maxima (red rectangles) only show a very slight S-shape with its minimum at 40 K (indicated by the red dashed line) spanning across the more narrow temperature range from 20 K to 100 K. In a straightforward approximation, the PL-maxima for the type-II and W-type samples can be assumed to be a linear superposition of the properties of the corresponding type-I reference QWs. Both the electron density-of-states (eDOS) and hole density-of-states (hDOS) should influence the spatially indirect transition between two different layers. The experimental findings support this picture for both the type-II and the W-type

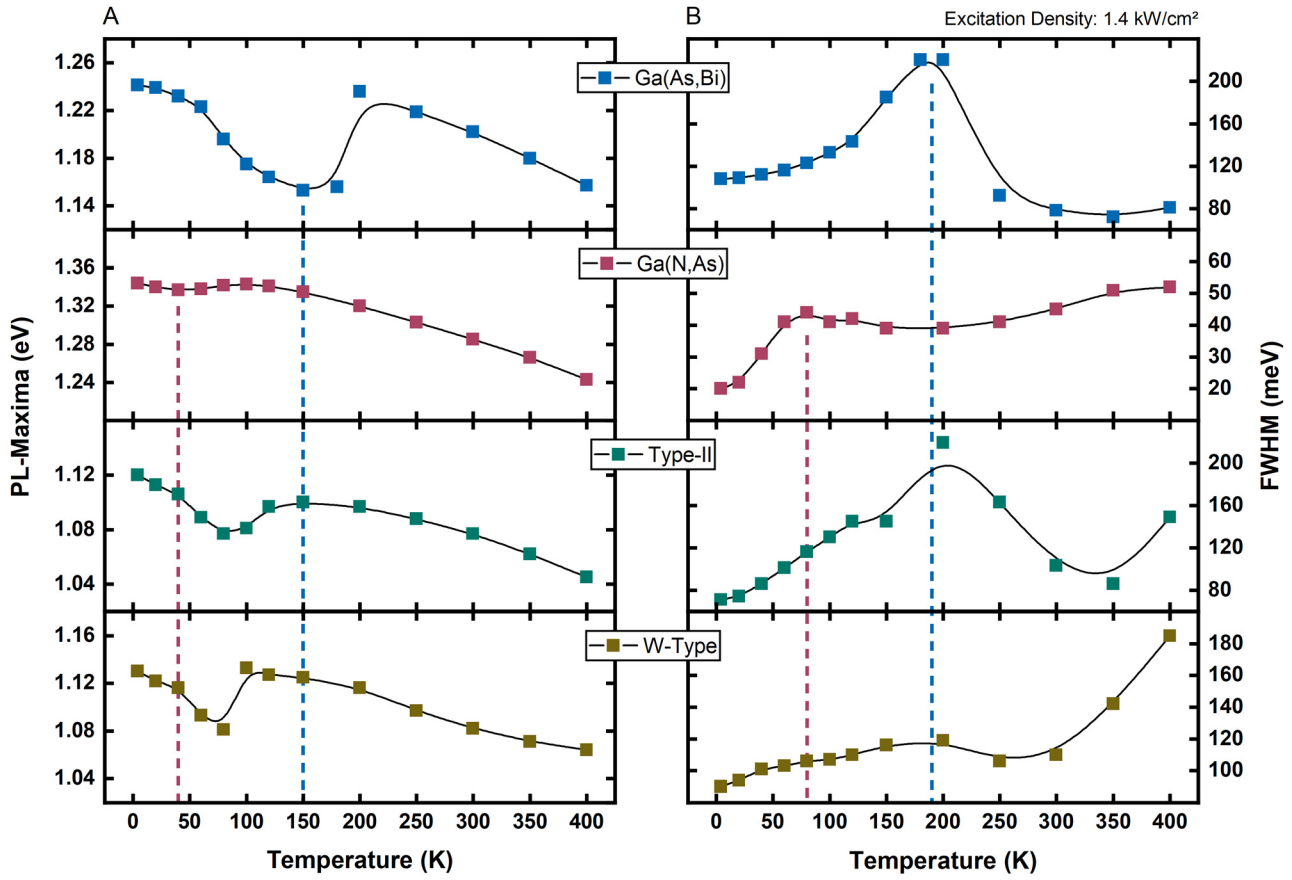

FIG. 2. Temperature dependency of the PL-maxima (a) and FWHM (b) is plotted as rectangles. The black lines are guides to the eye, while the dashed lines indicate the disorder-induced local minima (maxima) of the Ga(N,As) reference samples (red) and Ga(As,Bi) reference samples (blue) PL-maxima (FWHM).

samples. Here, the S-shape has its minimum at a temperature of 80 K and closely resembles the findings for the Ga(N,As) layer regarding the temperature shift of the PL peak position. The temperature of the local minimum of the S-shape is defined by the mobility edge of the carriers. Thus, symmetrizing the layer arrangement by introducing a second Ga(N,As) layer leads to a decrease in the mobility edge. The disorder of the Ga(As,Bi) layer influences the width of the S-shape. Nonetheless, the S-shape is more narrow for the type-II and W-type samples than for the Ga(As,Bi) QW sample. The direct comparison of the data for the type-II and the W-type sample reveals that the S-shape of the W-type sample appears to be influenced more by the Ga(N,As) layer. Two mechanisms can explain such a behavior. On the one hand, the electron wave functions are mostly located in the Ga(N,As) layers and will leak well into the Ga(As,Bi) layer by design, while the hole wave functions are well confined in the Ga(As,Bi) layer. The electron wave function in the asymmetric arrangement, however, has less overlap with the hole wave function in the Ga(As,Bi) layer than in a symmetric arrangement. On the other hand, we need to consider the joint densities-of-states for both types of heterostructures. This becomes evident when considering the combined densities-of-states for both types of heterostructures. While the asymmetric type-II structure consists of one electron-Ga(N,As) layer and one hole-Ga(As,Bi) layer, the symmetric W-type structure has two electron-Ga(N,As) layers. Both Ga(N,As) layers are not perfectly identical due to growth constraints and we have to include the possibility for nondegenerate states. Accordingly, the joint DOS for the type-II sample can be expressed approximately as $eDOS_{Ga(N,As)} \cdot hDOS_{Ga(As,Bi)}$, while the second Ga(N,As) layer has to be taken into account for the W-type structure yielding $eDOS_{Ga(N,As)modified} \cdot hDOS_{Ga(As,Bi)}$. Here, $eDOS_{Ga(N,As)modified}$ includes changes in the electron-DOS originating from the additional Ga(N,As) layer. This explains the differences observed for the samples with symmetric and the asymmetric type-II transition, respectively. PLE measurements confirm these assumptions and will be discussed below.

The analysis of the FWHM provides additional information on the electronic properties. The FWHM is shown in Fig. 2(b). Similar to the PL-maxima, the Ga(As,Bi) structure shows the strongest disorder features. The FWHM has its maximum at 190 K (indicated by the blue dashed line). The Ga(N,As) QW FWHM peaks at 80 K (red dashed line). Again for both, the type-II sample and W-type sample, the FWHM reassembles the FWHM line shape of the type-I QWs. However, the FWHM is dominated by the linewidth of the Ga(As,Bi). The electrons and holes are more separated in the asymmetric type-II

structure than in the symmetric type-II structure, as the former shows weaker confinement due to the wider Ga(N,As) layer width. The resulting difference in wavefunction overlap leads to different temperature ranges in which electrons and holes become mobile, as the corresponding wave functions have their maxima in the Ga(N,As) and Ga(As,Bi) layers, respectively. The PL spectra shown in Fig. 1 already hint different ensembles of tail states for the Ga(N,As) and the Ga(As,Bi) QW sample. The tail states of the Ga(As,Bi) layer should influence the emission of the type-II transition tremendously, due to the known disorder in the Ga(As,Bi) valence bands.[27] Temperatures above 300 K are most relevant for device operation. Here, a clear difference between the type-I and type-II samples emerges. The FWHM of the type-II and W-type samples increases rapidly in contrast to the type-I samples, which show an expected increase in the FWHM according to the carrier distribution as a function of the temperature. Most likely, the increase in the FWHM above 300 K observed for the type-II and W-type samples originates in additional transitions[31] between electron states in the Ga(N,As) layer and higher hole states in the Ga(As,Bi) layer.

The comparison of the data from the type-II sample and the W-type sample reveals a different weighting of Ga(As,Bi) and Ga(N,As) signatures in the temperature dependence of the PL. The influence of the Ga(As,Bi) disorder signatures is decreased with the introduction of a second Ga(N,As) layer. In order to further analyze the tail states of the structures, we perform excitation-density-dependent PL measurements.

The reasoning of localized states is an exponential density of states. This is illustrated in Fig. 3(a). The arrow indicates the shift of the PL maximum, while the shaded area draws the saturated states. Higher excitation-densities result in occupation of more and more of the localized states. Therefore, the PL-maximum shifts toward higher energies as a result of this state filling process.[30] The PL-maxima at 4 K as a function of excitation density are plotted in Fig. 3(b) for the type-II structures. We observe an exponential behavior of the PL-maxima for both samples. Within our experimentally accessible range, the excitation-density-dependent PL measurements expose a shift of the PL-maxima of 50 meV and 78 meV for the asymmetric and symmetric structure, respectively. This means that the slope of the DOS in the probed regime increases slower in the case of the W-type sample. We attribute this higher impact of disorder to the aforementioned differences in the two Ga(N,As) layers of the W-type structure. The PL-maxima of the reference samples are shown in Fig. 3(c) instead. The PL-maxima shift is 16 meV and 50 meV for the Ga(N,As) QW and the Ga(As,Bi) QW, respectively. Therefore, the results indicate the major role of localized states in the Ga(As,Bi) hole-layer on the disorder properties of the type-II transition. Additionally, this is in good agreement with the previous assumption that the influence on the FWHM of the Ga(As,Bi) layer originates in the tail states of the joint DOS. Within the low excitation regime, the results show that the low-energy tail states of the Ga(As,Bi) layer influence the emission of the type-II transition, since they enable transitions from excited states into localized states in the band tails.

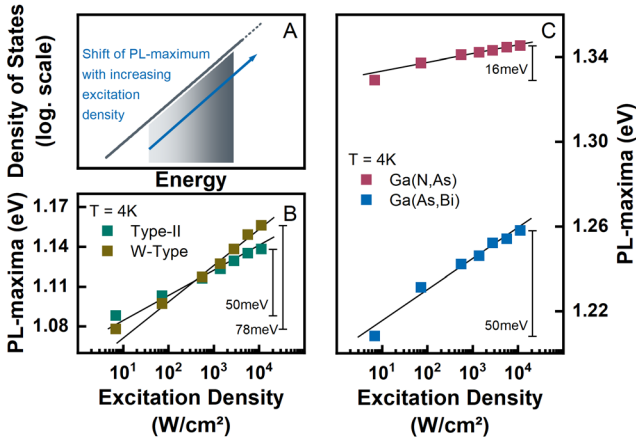

FIG. 3. The correlation between an exponential DOS and the excitation-density dependent shift of the PL-maxima is illustrated in (a). The shaded area indicates the increasing excitation density, while the blue arrow indicates the shift of the PL-maxima. The excitation-density-induced shifts of the PL-maxima at 4 K are drawn as scatter plots for the type-II structures (b) and the reference samples (c).

PLE data reveal the carrier recombination paths in type-II structures. Notably, PLE data are complex as they contain information about the absorption process, relaxation pathways, and recombination probabilities.[32] Hence, it contains information on the joint DOS and reveals which layers contribute most in feeding the spatially indirect transition in the heterostructures. Figure 4 shows PL and PLE data at a lattice temperature of 4 K as the solid line and shaded area, respectively. An additional set of PL data is taken using the super continuum laser at an emission energy of 2.33 eV (532 nm) to relate PL and PLE data. Figure 4(a) displays the spectra of the asymmetric type-II structure, and the data of the symmetric W-type structure are plotted in Fig. 4(b). Both samples have similar PL features. At 1.5 eV, the GaAs layer luminescence is detected followed by some nitrogen cluster states around 1.4 eV (Ref. 33) and the PL of the type-II transition at 1.1 eV. The dashed vertical line indicates the detection energy for the PLE measurements. While the PL line shapes are quite similar, the PLE spectra of the asymmetric and symmetric structures reveal some distinct differences. Naively, two low-energy peaks originating from the Ga(N,As) and the Ga(As,Bi) layer are expected in addition to the pronounced increase for energies above 1.5 eV associated with GaAs. Both the asymmetric and symmetric samples show a signal below energies of the GaAs regime. This signature of the Ga(N,As) layer exhibits well-known effects like Coulomb-enhancement for energies above the exciton resonances.[34] For the symmetric W-type structure, the low-energy tail of the resonance at 1.35 eV is much steeper. In addition, the resonance itself seems to be sharper than for the asymmetric structure. Again, we attribute this to the stronger carrier confinement, which results in higher absorption,[35] and to the above discussed changes in the joint DOS. The energy regime below the Ga(N,As) signature features an additional signature at approximately 1.25 eV, which is attributed to the Ga(As,Bi) layer. The PLE signal of the Ga(As,Bi) layer for the symmetric type-II arrangement below the Ga(N,As) layer energy regime is barely observable and clearly less intense than that of the asymmetric type-II arrangement. This behavior is explained by the nature of light absorption in QWs: (1) thinner QWs show stronger absorption due to the stronger carrier confinement and (2) the absorption of QWs does not depend on the amount of material but on the number of QWs.[35] Thus, for the asymmetric type-II structure, the weaker PLE signature of the Ga(As,Bi) layer can be attributed to the stronger inhomogeneous broadening, which was already observed in the temperature-dependent measurements. The

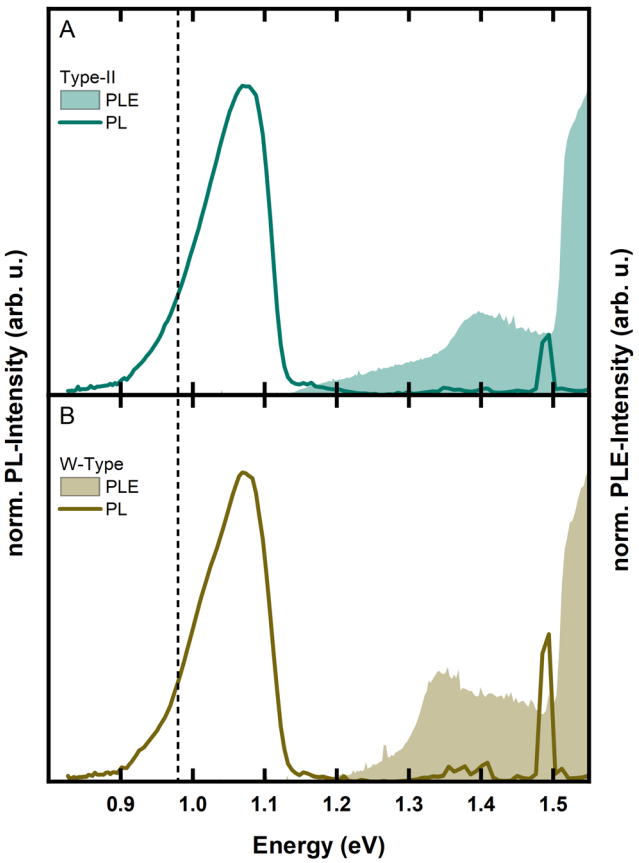

FIG. 4. Normalized PLE (shaded area) and normalized PL (solid line) data are plotted for the asymmetric (a) and symmetric (b) type-II samples. The dashed line indicates the detection energy used for the PLE measurements.

symmetric W-type structure consists of two Ga(N,As) layers, which contribute to the absorption process. Thus, the intensity of the Ga(As,Bi) layer signature compared to that of the Ga(N,As) layer signature is weaker in the W-type arrangement. The PLE data confirm the hypothesis that the changes in the combined DOS introduced by the second Ga(N,As) layer lead to these differences in PL and PLE spectra. The rather weak signature of the Ga(As,Bi) layers suggests that the electrons excited directly in the Ga(As,Bi) layer contribute insignificantly to the recombination via the type-II transition in both cases. The carriers recombining via the type-II transition are excited mostly in the GaAs barriers or in the Ga(N,As) electron-layers. We, hence, assume that the carriers excited directly in the Ga(As,Bi) layers are mostly trapped in localized states and, thus, cannot contribute to the type-II transition.

In summary, the analysis of the disorder signatures and the carrier recombination paths allows a clear distinction between the influences of the disorder properties of the emission of the two species of layers on the type-II recombination. The Ga(N,As) and Ga(As,Bi) layers feature a distinct behavior regarding their temperature-dependency of both PL maximum and FWHM. The spatially indirect transition for both the symmetric and asymmetric layer configurations inherits properties evident for the type-I reference quantum wells. This enables an assignment of the influence of the layers' materials properties on the type-II recombination. For both spatially indirect samples, the electron layers mainly influence the PL maxima dependence on temperature and excitation density, while the hole layers influence the corresponding FWHM. These results are in good agreement with straight-forward considerations taking into account that holes feature larger effective masses than electrons and are, hence, more confined in the Ga(As,Bi) layer. Thus, they have less impact on the recombination across the interface. Excitation-density-dependent PL data reveal the origin of the disorder signatures as localized tail states in the Ga(As,Bi) hole layers. The Ga(N,As) electron layer influences the symmetric W-type heterostructure more than the asymmetric one. These observations are conclusively explained when considering the respective DOS'. The carriers excited in the Ga(N,As) layer and GaAs barrier contribute more to the type-II transition than the Ga(As,Bi) layer. The valence bands of the latter are dominated by localized states. Thus, the charge carriers created directly in the Ga(As,Bi) layer are trapped in these states and, hence, contribute less to the recombination across the type-II interface.

Our results provide important implications for lasing applications utilizing such W-type arrangements. The rise of the FWHM at temperatures above 300 K is crucial for the minimum threshold current needed for lasing, since it increases the amount of states that have to be filled before reaching the inversion regime. A stronger carrier confinement in the electron and hole layers can probably shift the higher order type-II transitions out of the operation temperature regime of future devices. Nonetheless, at higher carrier densities, we expect these Ga(N,As)/Ga(As,Bi) heterostructures to perform more efficient, since disorder plays a minor role and the stronger electrostatic attraction between electrons and holes in adjacent layers improves their spatial overlap.

This work was supported by the German Research Foundation (GRK 1782: Functionalization of Semiconductors) and the Center for Materials Research (No. ZfM/LaMa). S.C. acknowledges support through the Heisenberg program (No. CH660/8).

DATA AVAILABILITY

The data that support the findings of this study are available from the corresponding author upon reasonable request.

REFERENCES

[1]G. N. Childs, S. Brand, and R. A. Abram, "Intervalence band absorption in semiconductor laser materials," Semicond. Sci. Technol. **1**, 116–120 (1986).
[2]S. J. Sweeney, A. R. Adams, M. Silver, E. P. O'Reilly, J. R. Watling, A. B. Walker, and P. J. A. Thijs, "Dependence of threshold current on QW position and on pressure in 1.5 μm InGaAs(P) lasers," Phys. Status Solidi B **211**, 525 (1999).
[3]A. D. Andreev and E. P. O'Reilly, "Theoretical study of Auger recombination in a GaInNAs 1.3 μm quantum well laser structure," Appl. Phys. Lett. **84**, 1826 (2004).
[4]G. G. Zegrya and A. D. Andreev, "Mechanism of suppression of Auger recombination processes in type-II heterostructures," Appl. Phys. Lett. **67**, 2681 (1995).
[5]G. G. Zegrya and A. F. Andreev, "Theory of the recombination of nonequilibrium carriers in type-II heterostructures," J. Exp. Theor. Phys. **82**, 2 (1996).
[6]W. Walukiewicz and J. M. O. Zide, "Highly mismatched semiconductor alloys: From atoms to devices," J. Appl. Phys. **127**, 010401 (2020).

[7]T. Hepp, O. Maßmeyer, D. A. Duffy, S. J. Sweeney, and K. Volz, "Metalorganic vapor phase epitaxy growth and characterization of quaternary (Ga,In) (As,Bi) on GaAs substrates," J. Appl. Phys. **126**, 85707 (2019).
[8]C. A. Broderick, M. Usman, E. P. O'Reilly, W. Xiong, and S. J. Sweeney, "Band engineering in dilute nitride and bismide semiconductor lasers," Semicond. Sci. Technol. **27**, 094011 (2012).
[9]J. Veletas, T. Hepp, K. Volz, and C. Chatterjee, "Bismuth surface segregation and disorder analysis of quaternary (Ga,In)(As,Bi)/InP alloys," J. Appl. Phys. **126**, 135705 (2019).
[10]P. Ludewig, N. Knaub, N. Hossain, S. Reinhard, L. Nattermann, I. P. Marko, S. R. Jin, K. Hild, S. Chatterjee, W. Stolz, S. J. Sweeney, and K. Volz, "Electrical injection Ga(AsBi)/(AlGa)As single quantum well laser," Appl. Phys. Lett. **102**, 242115 (2013).
[11]S. Francoeur, M.-J. Seong, A. Mascarenhas, S. Tixier, M. Adamcyk, and T. Tiedje, "Band gap of GaAsBi, $0 < x < 3.6\%$," Appl. Phys. Lett. **82**, 3874 (2003).
[12]S. Tixier, M. Adamcyk, T. Tiedje, S. Francoeur, A. Mascarenhas, P. Wei, and F. Schiettekatte, "Molecular beam epitaxy growth of $GaAs_{1-x}Bi_x$," Appl. Phys. Lett. **82**, 2245 (2003).
[13]N. A. Riordan, C. Gogineni, S. R. Johnson, X. Lu, T. Tiedje, D. Ding, Y. H. Zhang, R. Fritz, K. Kolata, S. Chatterjee, K. Volz, and S. W. Koch, "Temperature and pump power dependent photoluminescence characterization of MBE grown GaAsBi on GaAs," J. Mater. Sci. **23**, 1799 (2012).
[14]J. Hader, S. C. Badescu, L. C. Bannow, J. V. Moloney, S. R. Johnson, and S. W. Koch, "Extended band anti-crossing model for dilute bismides," Appl. Phys. Lett. **112**, 062103 (2018).
[15]K. Alberi, O. D. Dubon, W. Walukiewicz, K. M. Yu, K. Bertulis, and A. Krotkus, "Valence band anticrossing in $GaBi_xAs_{1-x}$," Appl. Phys. Lett. **91**, 051909 (2007).
[16]S. Imhof, C. Bückers, A. Thränhardt, J. Hader, J. V. Moloney, and S. W. Koch, "Microscopic theory of the optical properties of Ga(AsBi)/GaAs quantum wells," Semicond. Sci. Technol. **23**, 125009 (2008).
[17]K. Alberi, J. Wu, W. Walukiewicz, K. M. Yu, O. D. Dubon, S. P. Watkins, C. X. Wang, X. Liu, Y.-J. Cho, and J. Furdyna, "Valence-band anticrossing in mismatched III-V semiconductor alloys," Phys. Rev. B **75**, 045203 (2007).
[18]P. J. Klar, H. Grüning, W. Heimbrodt, J. Koch, F. Höhnsdorf, W. Stolz, P. M. A. Vicente, and J. Camassel, "From N isoelectronic impurities to N-induced bands in the GaN_xAs_{1-x} alloy," Appl. Phys. Lett. **76**, 3439 (2000).
[19]W. Shan, W. Walukiewicz, K. M. Yu, J. W. Ager, E. E. Haller, J. F. Geisz, D. J. Friedman, J. M. Olson, S. R. Kurtz, H. P. Xin, and C. W. Tu, "Band anticrossing in III-N-V alloys," Phys. Status Solidi B **223**, 75 (2001).
[20]T. Taliercio, R. Intartaglia, B. Gil, P. Lefebvre, T. Bretagnon, U. Tisch, E. Finkman, J. Salzman, M.-A. Pinault, M. L. Gt, and E. Tournié, "From GaAs:N to oversaturated GaAsN: Analysis of the band-gap reduction," Phys. Rev. B **69**, 73303 (2004).
[21]C. A. Broderick, S. Jin, I. P. Marko, K. Hild, P. Ludewig, Z. L. Bushell, W. Stolz, J. M. Rorison, E. P. O'reilly, K. Volz, and S. J. Sweeney, "$GaAs_{1-x}Bix/GaNyAs_{1-y}$ type-II quantum wells: Novel strain-balanced heterostructures for GaAs-based near- and mid-infrared photonics," Sci. Rep. **7**, 1–9 (2017).
[22]S. Francoeur, S. Tixier, E. Young, T. Tiedje, and A. Mascarenhas, "Bi isoelectronic impurities in GaAs," Phys. Rev. B **77**, 085209 (2008).
[23]C. Gogineni, N. A. Riordan, S. R. Johnson, X. Lu, and T. Tiedje, "Disorder and the Urbach edge in dilute bismide GaAsBi," Appl. Phys. Lett. **103**, 041110 (2013).
[24]S. D. Baranovskii, R. Eichmann, and P. Thomas, "Temperature-dependent exciton luminescence in quantum wells by computer simulation," Phys. Rev. B **58**, 13081 (1998).
[25]C. Karcher, K. Jandieri, B. Kunert, R. Fritz, M. Zimprich, K. Volz, W. Stolz, F. Gebhard, S. D. Baranovskii, and W. Heimbrodt, "Peculiarities of the photoluminescence of metastable Ga(N,As,P)/GaP quantum well structures," Phys. Rev. B **82**, 245309 (2010).
[26]V. Valkovskii, K. Jandieri, F. Gebhard, and S. D. Baranovskii, "Rethinking the theoretical description of photoluminescence in compound semiconductors," J. Appl. Phys. **123**, 055703 (2018).
[27]S. Imhof, A. Thränhardt, A. Chernikov, M. Koch, N. S. Köster, K. Kolata, S. Chatterjee, S. W. Koch, X. Lu, S. R. Johnson, D. A. Beaton, T. Tiedje, and O. Rubel, "Clustering effects in Ga(AsBi)," Appl. Phys. Lett. **96**, 131115 (2010).
[28]S. Imhof, C. Wagner, A. Thränhardt, A. Chernikov, M. Koch, N. S. Köster, S. Chatterjee, S. W. Koch, O. Rubel, X. Lu, S. R. Johnson, D. A. Beaton, and T. Tiedje, "Luminescence dynamics in Ga(AsBi)," Appl. Phys. Lett. **98**, 161104 (2011).
[29]M. K. Shakfa, D. Kalincev, X. Lu, S. R. Johnson, D. A. Beaton, T. Tiedje, A. Chernikov, S. Chatterjee, and M. Koch, "Quantitative study of localization effects and recombination dynamics in GaAsBi/GaAs single quantum wells," J. Appl. Phys. **114**, 164306 (2013).
[30]V. Valkovskii, M. K. Shakfa, K. Jandieri, P. Ludewig, K. Volz, W. Stolz, M. Koch, and S. D. Baranovskii, "Excitation dependence of the photoluminescence lineshape in Ga(NAsP)/GaP multiple quantum well: Experiment and Monte-Carlo simulation," J. Phys. D **50**, 025105 (2017).
[31]S. Gies, C. Kruska, C. Berger, P. Hens, C. Fuchs, A. Ruiz Perez, N. W. Rosemann, J. Veletas, S. Chatterjee, W. Stolz, S. W. Koch, J. Hader, J. V. Moloney, and W. Heimbrodt, "Excitonic transitions in highly efficient (GaIn)As/Ga(AsSb) type-II quantum-well structures," Appl. Phys. Lett. **107**, 182104 (2015).
[32]M. Cardona and P. Y. Yu, *Fundamentals of Semiconductors*, 4th ed. (Springer, 1995).
[33]A. Lindsay and E. P. O'reilly, "Unification of the band anticrossing and cluster-state models of dilute nitride semiconductor alloys," Phys. Rev. Lett. **93**, 196402 (2004).
[34]H. Haug and S. W. Koch, *Quantum Theory of the Optical and Electronic Properties of Semiconductors* (World Scientific Publishing, 2003).
[35]P. Blood, "On the dimensionality of optical absorption, gain, and recombination in quantum-confined structures," J. Quantum Electron. **36**, 354 (2000).